Ribosomal frameshifting and dual-target antiactivation restrict quorum-sensing–activated transfer of a mobile genetic element

Joshua P. Ramsay[a,b,1], Laura G. L. Tester[a], Anthony S. Major[a], John T. Sullivan[a], Christina D. Edgar[c], Torsten Kleffmann[c], Jackson R. Patterson-House[b], Drew A. Hall[b], Warren P. Tate[c], Michael F. Hynes[d], and Clive W. Ronson[a]

Departments of [a]Microbiology and Immunology and [c]Biochemistry, University of Otago, Dunedin 9016, New Zealand; [b]Curtin Health Innovation Research Institute Biosciences Precinct, Faculty of Health Sciences, Curtin University, Bentley, WA 6102, Australia; and [d]Department of Biological Sciences, University of Calgary, Calgary, AB T2N 1N4, Canada

Edited by E. Peter Greenberg, University of Washington, Seattle, WA, and approved February 25, 2015 (received for review January 27, 2015)

Symbiosis islands are integrative and conjugative mobile genetic elements that convert nonsymbiotic rhizobia into nitrogen-fixing symbionts of leguminous plants. Excision of the *Mesorhizobium loti* symbiosis island ICE*Ml*Sym^{R7A} is indirectly activated by quorum sensing through TraR-dependent activation of the excisionase gene *rdfS*. Here we show that a +1 programmed ribosomal frameshift (PRF) fuses the coding sequences of two TraR-activated genes, *msi172* and *msi171*, producing an activator of *rdfS* expression named Frameshifted excision activator (FseA). Mass-spectrometry and mutational analyses indicated that the PRF occurred through +1 slippage of the tRNA^{phe} from UUU to UUC within a conserved *msi172*-encoded motif. FseA activated *rdfS* expression in the absence of ICE*Ml*Sym^{R7A}, suggesting that it directly activated *rdfS* transcription, despite being unrelated to any characterized DNA-binding proteins. Bacterial two-hybrid and gene-reporter assays demonstrated that FseA was also bound and inhibited by the ICE*Ml*Sym^{R7A}-encoded quorum-sensing antiactivator QseM. Thus, activation of ICE*Ml*Sym^{R7A} excision is counteracted by TraR antiactivation, ribosomal frameshifting, and FseA antiactivation. This robust suppression likely dampens the inherent biological noise present in the quorum-sensing autoinduction circuit and ensures that ICE*Ml*Sym^{R7A} transfer only occurs in a subpopulation of cells in which both *qseM* expression is repressed and FseA is translated. The architecture of the ICE*Ml*Sym^{R7A} transfer regulatory system provides an example of how a set of modular components have assembled through evolution to form a robust genetic toggle that regulates gene transcription and translation at both single-cell and cell-population levels.

quorum sensing | antiactivator | ribosomal frameshift | ICE | horizontal gene transfer

Integrative and conjugative elements (ICEs) are the most abundant conjugative DNA elements found in prokaryotes (1). They reside integrated within the host's genome, but are able to excise as circular elements and transfer to other cells by conjugation (2). ICEs carry a diverse range of genetic cargo, including antimicrobial-resistance, virulence, metabolism, and symbiosis determinants (3–6). Nevertheless, from the perspective of regulation of horizontal transfer, ICEs remain the least-studied mobile elements, in part due to the paucity of experimentally amenable ICEs that can be transferred to recipients under laboratory conditions. In particular, the regulatory and environmental factors that influence the switch from vertical inheritance of ICEs to horizontal transfer to other cells are poorly understood for most ICEs.

The symbiosis island of *Mesorhizobium loti* strain R7A, ICE*Ml*Sym^{R7A}, is a 502-kb ICE, discovered through its ability to convert nonsymbiotic mesorhizobia into N_2-fixing symbionts of legumes of the genus *Lotus* (7, 8). Excision and integration of ICE*Ml*Sym^{R7A} are catalyzed by the integrase IntS, but excision from the chromosome is stimulated only after expression of the excisionase RdfS (9). Several regulatory elements that influence excision and transfer of ICE*Ml*Sym^{R7A} have been identified, including TraR, a LuxR-family quorum-sensing (QS) regulator that activates gene transcription in response to *N*-acyl-homoserine-lactones (AHLs) produced by TraI1 (10, 11). However, the direct regulators of *rdfS* expression have not been identified. Two hypothetical ORFs, *msi172* and *msi171*, are primary candidates, because their expression is activated by TraR and they are essential for transfer (11).

TraR is generally inactive in *M. loti* cells, even in the presence of excess AHL, due to inhibition by an antiactivator, QseM (10, 11). Unexpectedly, overexpression of QseM represses ICE*Ml*Sym^{R7A} excision to levels below those observed in wild type or in a strain carrying a deletion of *traR*, suggesting that QseM is able to repress *rdfS* expression by a mechanism in addition to its effect on TraR activity (10). The expression of *qseM* is controlled by the concentration-dependent DNA binding of a transcriptional regulator, QseC, to a pair of operator sequences overlapping the *qseC* and *qseM* promoters, potentially leading to repression of *qseM* expression and activation of ICE*Ml*Sym^{R7A} transfer in only a minority of cells.

Significance

Integrative and conjugative elements (ICEs) facilitate horizontal transfer of multiple genetic determinants. Here we show that a programmed ribosomal frameshift (PRF) contributes to the regulation of ICE transfer. The low-frequency PRF fuses the coding sequences of two genes, resulting in a single-protein Frameshifted excision activator (FseA) that activates ICE excision. An antiactivator, QseM, known to disrupt the quorum-sensing regulator TraR, also disrupted FseA. The evolved PRF site, together with the dual-target antiactivator, QseM, likely provides robust suppression of ICE transfer in the face of the inherent biological noise of quorum-sensing autoinduction. This work illustrates how a complex multipartite regulatory system has assembled through evolution to form a robust genetic toggle to control gene transcription and translation at both single-cell and cell-population levels.

Author contributions: J.P.R., J.T.S., T.K., W.P.T., M.F.H., and C.W.R. designed research; J.P.R., L.G.L.T., A.S.M., J.T.S., C.D.E., T.K., J.R.P.-H., D.A.H., and M.F.H. performed research; C.D.E., T.K., and W.P.T. contributed new reagents/analytic tools; J.P.R., L.G.L.T., A.S.M., J.T.S., C.D.E., T.K., W.P.T., M.F.H., and C.W.R. analyzed data; J.P.R., J.T.S., T.K., W.P.T., M.F.H., and C.W.R. wrote the paper; and J.P.R., J.T.S., W.P.T., M.F.H., and C.W.R. supervised students.

The authors declare no conflict of interest.

This article is a PNAS Direct Submission.

[1]To whom correspondence should be addressed. Email: joshramsay@gmail.com.

This article contains supporting information online at www.pnas.org/lookup/suppl/doi:10.1073/pnas.1501574112/-/DCSupplemental.

The predicted products of *msi172*, *msi171*, and *qseM* show no sequence similarity to structurally characterized proteins. However, they are conserved on numerous ICEs found throughout the proteobacteria, most of which lack recognizable QS loci. Interestingly, homologs of Msi172 and Msi171 are often encoded as a single ORF (11). In this study, we report that the functional product of the *msi172* and *msi171* ORFs—named here Frameshifted excision activator (FseA)—is produced through a programmed ribosomal frameshift (PRF) and directly activates the *rdfS* promoter. Furthermore, we found that QseM is a dual-target antiactivator that, in addition to binding TraR, binds and inhibits FseA, thus explaining the repression of excision by QseM in the absence of TraR. Together, the dual-target antiactivator and PRF have likely evolved to suppress the inherent biological noise present in the QS autoinduction circuit and ensure that ICE*Ml*Sym^{R7A} excision is not spuriously induced, and only occurs in a subset of cells in the population.

Results

A Product of *msi172–msi171* Induces Expression from the *rdfS* Promoter. Constitutive expression of the ICE*Ml*Sym^{R7A} excisionase gene *rdfS* causes growth inhibition that can be partially relieved by curing of ICE*Ml*Sym^{R7A} (9). Attempts to introduce a plasmid constitutively expressing *msi172–msi171* into *M. loti* strain R7A were unsuccessful (11), suggesting that they might activate *rdfS* expression. The *rdfS* gene is located upstream of genes encoding TraF (TrbC protease) and a predicted murein hydrolase, Msi107 (9, 10). 5′ RACE analysis of the *rdfS–traF–msi107* transcript from R7AΔ*qseM* revealed transcription initiated 28–30 bp upstream of *rdfS* (Fig. S1*A*). An inverted repeat, GGCGAA-N_{16}-TTCGCC, was located directly upstream of the −35 region, and an identical motif was present upstream of *rdfS* homologs in *Mesorhizobium alhagi*, *Mesorhizobium ciceri*, and *Parvibaculum lavamentivorans* (Fig. S1*B*).

To measure expression from the *rdfS* promoter, a stable low-copy broad-host-range plasmid pSDZ was constructed that carried a promoterless *lacZ* gene and a divergently oriented *lac* promoter (Fig. S2). The *rdfS* promoter was cloned upstream of *lacZ*, producing pSDrdfS–lacZ, and the *msi172–msi171* region was cloned downstream of the *lac* promoter in pSDrdfS–lacZ, producing p172171rdfS–lacZ (Fig. S1*D*). Both plasmids were introduced into strain R7A and its ICE*Ml*Sym^{R7A}-cured derivative R7ANS. Growth of R7A(p172171rdfS–lacZ) was inhibited with the addition of 0.1 mM isopropyl beta-D-thiogalactoside (IPTG), whereas growth of R7A(pSDrdfS–lacZ) was unaffected. Neither of the constructs conferred IPTG-dependent growth inhibition on R7ANS, confirming that growth inhibition only occurred when ICE*Ml*Sym^{R7A} was present. *rdfS* promoter expression was examined in R7ANS containing pSDrdfS–lacZ or p172171rdfS–lacZ by assaying β-galactosidase activity in the presence of 0.1 mM IPTG. The *rdfS* promoter was weakly expressed from both constructs, but expression was significantly higher from p172171rdfS–lacZ [1.63 relative fluorescence units (RFU)/s per OD_{600} vs. 0.44 RFU/s per OD_{600} ($P = 0.006$)] (Fig. S3*A*). Thus, a product(s) of the *msi172–msi171* region induced expression from the *rdfS* promoter, and other genes located on ICE*Ml*Sym^{R7A} were not required.

The FseA Transcriptional Activator Is Produced from *msi172* and *msi171* by a +1 Programmed Ribosomal Frameshift. *msi172* and *msi171* homologs are present on 17 of 28 elements related to ICE*Ml*Sym^{R7A} that also encode homologs of RdfS and QseM (10). Further inspection revealed that Msi172 homologs were always encoded upstream of Msi171 homologs, and Msi171 sequences were usually (15/17) encoded in the adjacent +1 frame relative to Msi172. *msi172* homologs lacked conserved termination codons, and *msi171* homologs lacked conserved start codons or recognizable ribosome-binding sites (RBS). On two elements, *msi172* and *msi171* were found as a single ORF; moreover, they exist as a single ORF on the Tn*4371* family of ICEs that lack QseM homologs (Table S1) (10, 12). This combination of sequence features is common to PRF sites (13) and suggested that a PRF site might exist in the *msi172* mRNA that could promote the fusion of the Msi172 coding sequence with that of Msi171 during translation.

PRF events involve a slippage of the ribosome with respect to the mRNA during translation, resulting in a +1 or −1 shift in the reading frame. PRF sites often contain nucleotide sequence motifs that are highly conserved relative to the surrounding sequence (14, 15). Alignment of the nucleotide regions spanning the Msi172 and Msi171 homologs revealed that for 14 of 17 sequences, the 3′ end of the Msi172 gene contained a conserved sequence motif SRV.TGG.GGN.NTN.NNN.TTT.CSY (Fig. 1*A* and Table S1) upstream of the *msi172* stop codon. This motif encoded the slippery mRNA codon sequence UUU.CSY (UUU.CGC in *msi172*). Consecutive UUU.CNN codons are involved in the +1 slippage of tRNA^{phe} from one Phe codon UUU to the other Phe codon UUC in both mitochondrial and bacterial genes (15–17). Furthermore, a related motif with a slippery codon sequence UUU.UGC was identified near the 3′ end of nine *msi172* homologs in other *Mesorhizobium* strains (Table S1).

To test whether *msi172–msi171* functioned as a fused ORF, a T was deleted in the sequence TTT.CGC. This deletion produced a gene *fseA*, which encoded a protein identical to that which would be produced after the predicted +1 PRF at the UUU.CGC site (Fig. 1*B*). *fseA* was cloned into pSDrdfS–lacZ to give pFseArdfS–lacZ. We were unable to introduce pFseArdfS–lacZ into R7A, even in the absence of IPTG, suggesting that leaky expression from this vector strongly inhibited growth. β-galactosidase assays of R7ANS(pFseArdfS–lacZ) revealed that *rdfS* expression was ∼120-fold higher (194 RFU/s per OD_{600}) than that observed in R7ANS(p172171rdfS–lacZ) (Fig. S3*B*). Thus, FseA strongly activated the *rdfS* promoter, consistent with our hypothesis that a single product encoded by *msi172* and *msi171* activated ICE*Ml*Sym^{R7A} excision.

The PRF Occurs at Slippery Codon Sequence UUU.C. The PRF likely involved movement of tRNA^{phe} from UUU to UUC within the mRNA motif. Therefore, we reasoned that mutations that destroyed the UUC codon in the +1 frame would abolish frameshifting. The TTT.CGC sequence on p172171rdfS–lacZ was mutated to TTC.CGC, maintaining the tRNA^{phe} and tRNA^{arg} codons in the 0 frame and changing the second mRNA codon in the +1 frame from UUC (Phe) to UCC (Ser). In a second construct, TTT.CGC was changed to TTT.AGG, changing the second mRNA codon in the +1 frame to UUA (Leu) (Fig. 1*B*). Both mutations abolished expression from the *rdfS* promoter on p172171rdfS–lacZ (Fig. S3*A*), consistent with the proposed role of the UUC codon as the landing position of the tRNA^{phe} after the PRF event.

To confirm the position of the PRF site, a 340-bp fragment overlapping *msi172* and *msi171* was cloned between *malE* and *lacZ*α on pMAL-C2, so that a PRF would result in the fusion of maltose-binding protein (MBP) and LacZα. Expression was induced in *Escherichia coli*, and MBP-tagged products were isolated by using amylose-affinity chromatography. The major product was a 50-kDa protein corresponding to orthodox translational termination downstream of the PRF site (Fig. 1*C*). A minor 63-kDa product was also observed, corresponding in size to the predicted PRF product. Densitometry analysis indicated that the PRF occurred at a proportion of 4–5%. The expected site of frameshifting was confirmed by mass spectrometry of the 63-kDa protein (Fig. 1 *D–F*).

To see whether mRNA regions outside the identified conserved PRF motif were required for the PRF, complementary 42- to 43-bp oligonucleotides containing the conserved sequence region were cloned into pUC19, so that only a PRF event would result in translation of LacZα. Oligonucleotides carrying the ΔT229 deletion (as in *fseA*) or an additional stop codon in the +1 frame 6

MICROBIOLOGY

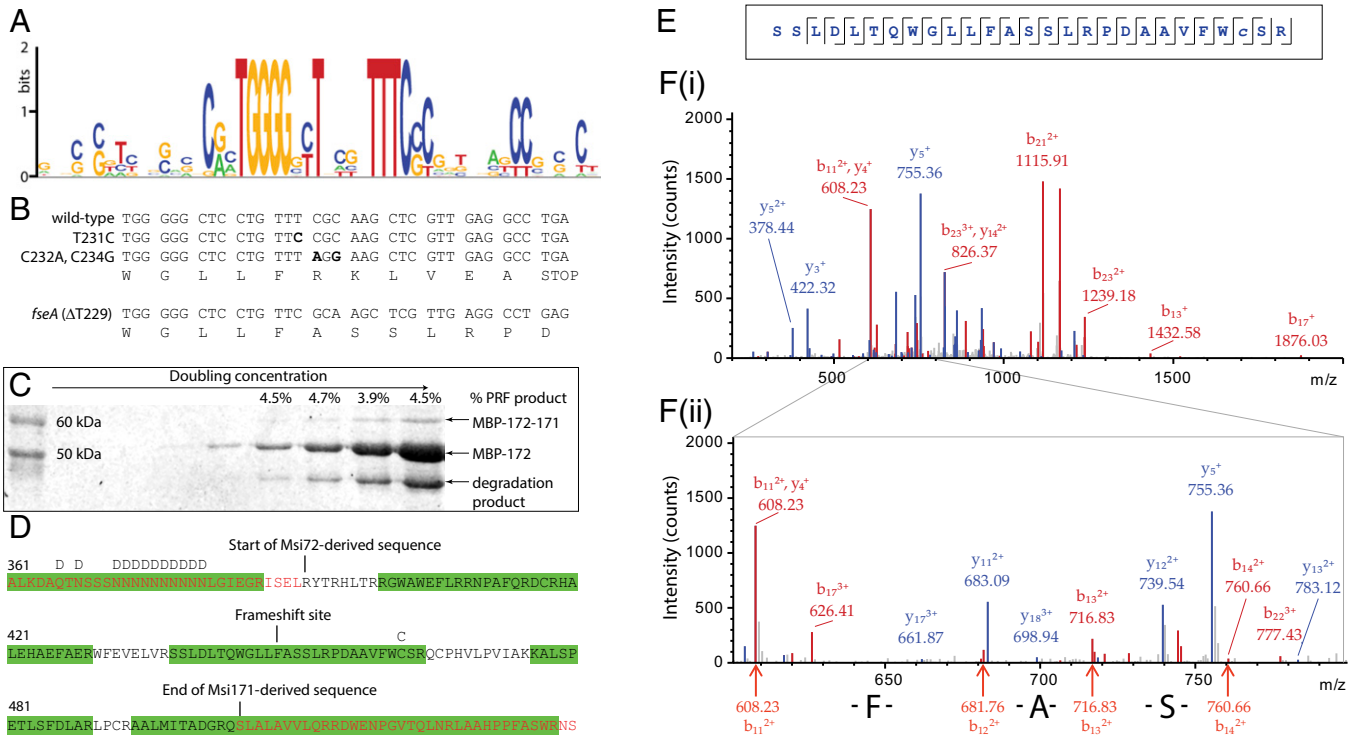

Fig. 1. Identification of the *msi172-msi171* PRF site. (*A*) DNA sequence conservation logo (18) constructed from an alignment of PRF sites found in *msi172–msi171* homologs (Table S1). (*B*) Mutations (bold) made in derivatives of p172171rdfS–lacZ. (*C*) Coomassie-stained SDS/PAGE gel of purified MBP–Msi172–Msi171–LacZα protein. The 63-kDa band is the frameshifted product, and the percentage abundance from the sum of both 50- and 60-kDa bands is presented above (estimated by densitometry). The sequence of each band was confirmed by mass spectrometry. A third, smaller product was identified as a MBP degradation product that terminated upstream of the *msi172*-encoded portion (not included in densitometry calculations). (*D*) Amino acid sequence spanning the MBP–Msi172–Msi171–LacZα junction of the frameshifted protein. Sequences identified by mass spectrometry are highlighted in green. Deamidated amino acids are indicated by "D" above the sequence, and cysteines modified by carboxyamidomethylation by "C." (*E*) Sequence of the tryptic peptide S438–R464 covering the site of frameshifting. Amino acids detected by fragment ions in the collision-induced dissociation (CID) spectrum are indicated by black lines pointing to the N terminus for fragment ions containing the N terminus (b-ions) and to the C terminus for fragment ions containing the C terminus (y-ions). (*F*) Annotated CID fragment spectrum of S438-R464 (*i*) and enlarged region of the spectrum showing the positively identified b-ions of the sequence FAS (*ii*).

nucleotides downstream of TTT.CGC were cloned as positive and negative controls, respectively. The positive control construct produced approximately one-third of the β-galactosidase activity of the pUC19 vector alone, suggesting that the amino acids encoded by the PRF site diminished β-galactosidase activity or stability. The construct carrying the wild-type *msi172–msi171* PRF produced 13% of the β-galactosidase activity of the positive control, whereas only a background level of expression (0.016% of positive control) was detected from the negative control construct (Fig. S4).

The TraR Antiactivator QseM Binds Msi172 and FseA and Inhibits FseA-Dependent Activation of the *rdfS* Promoter. Because *qseM* overexpression reduces excision (10), we wondered whether QseM directly repressed expression from the *rdfS* promoter. Plasmid pNQseM, carrying constitutively expressed *qseM* (10), was introduced into R7ANS(p172171rdfS–lacZ) and reduced expression from the *rdfS* promoter to background levels. Furthermore, pNQseM also repressed β-galactosidase activity from pFseArdfS–lacZ (Fig. S3*C*). This finding suggested that QseM was either able to directly bind the *rdfS* promoter or bind FseA and prevent FseA-dependent activation. We used the *E. coli* Bacteriomatch II bacterial two-hybrid assay (10), previously used to detect the interaction between QseM and *M. loti* TraR, to test for an interaction between QseM and FseA. Two-hybrid vector pTRG constructs carrying *msi172*, *msi172–msi171*, or *fseA* fused to RNA polymerase α, all produced strong interactions with the cI–QseM-expressing construct pBTqseM (10), whereas pTRG carrying only *msi171* did not (Fig. 2).

Discussion

Mobile genetic elements (MGEs) have evolved robust mechanisms to prevent spontaneous activation of horizontal gene transfer. The epigenetic maintenance of the phage λ lysogenic cycle, for example, is so stable that spontaneous entry into the lytic cycle will more likely result from mutation than abnormal repressor concentration (19). For an MGE, horizontal transfer is a high-risk strategy. Although an element can occasionally deliver itself to a fitter host through transfer, selection for this outcome only occurs afterward (20, 21). Most of the time, MGEs replicate vertically with their host, and their survival depends solely on the host's competitive fitness. To counter selection against their carriage, MGEs can endow hosts with genes that improve competitive fitness (22), encode selfish genetic modules that prevent their loss (23), and use exquisite regulatory systems that suppress the energetically costly process of transfer until optimal conditions arise (19). QS autoinduction circuits, such as the system that activates ICE*Ml*Sym^{R7A} excision and transfer (Fig. 3), are inherently prone to stochastic activation through fluctuations in gene transcription and autoinducer concentration (24, 25), resulting in unbridled activation. ICE*Ml*Sym^{R7A} has evolved an antiactivator, QseM, capable of completely suppressing QS. Indeed, in the absence of *qseM*, population-level activation of QS and excision occurs; however, in the presence of *qseM*, the addition of as much as 1 μM exogenous 3-oxo-C6-HSL does not induce expression from the *traI1* promoter (11). However, our previous investigations (9–11) suggested that additional layers of negative regulation existed that further suppressed activation of excision and transfer.

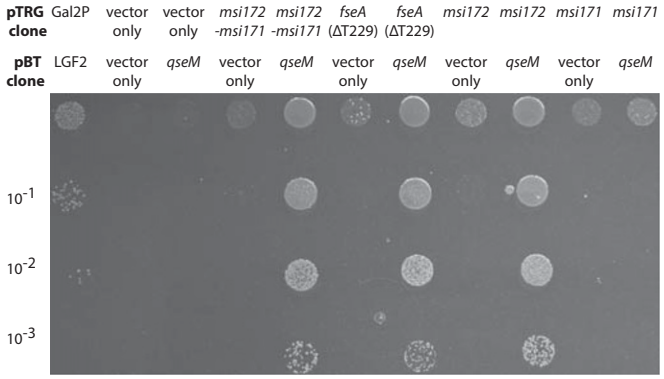

Fig. 2. Bacterial two-hybrid interaction assays of QseM with Msi172, Msi171, and FseA. Ten-microliter spots of 10-fold serial dilutions of cells into which two-hybrid plasmid constructs had been introduced by electroporation were spotted onto M9 minimal medium lacking histidine and containing 3-amino-1,2,4-triazole. Genes carried by the pTRG or pBT/pBTL vector are shown above each column of dilutions. Higher concentrations of colonies compared with the appropriate negative controls indicate in vivo protein–protein interactions. The positive control is shown in the first column. Numbers of colony-forming units per milliliter on selective and nonselective plates are provided in Table S2.

Excision and conjugative transfer of ICE*Ml*Sym^{R7A} are stimulated by TraR through the activation of *msi172–msi171* expression (11). Here we showed that the direct activator of *rdfS* expression is a PRF fusion protein, FseA, which is produced from a low-frequency +1 PRF event during translation of the *msi172* mRNA that brings *msi172* and *msi171* into the same translational reading frame. Furthermore, we demonstrated that the antiactivator QseM, which binds TraR and inhibits TraR-dependent activation of *traI2–msi172–msi171* expression (10, 11), also binds the *msi172*-encoded portion of FseA, preventing FseA-dependent activation of the *rdfS* promoter. Thus, QS-mediated activation of excision and transfer of ICE*Ml*Sym^{R7A} is prevented in most cells in a wild-type *M. loti* R7A population (9) through three distinct mechanisms: ribosomal frameshifting during translation of the *msi172* mRNA, antiactivation of TraR (and QS), and antiactivation of FseA (Fig. 3).

Programmed ribosomal frameshifting is a form of genetic recoding outside the constraints of the genetic code (26, 27). Although rare, it has been documented in all domains of life and can facilitate translation of single products from multiple ORFs, translation of multiple products from a single mRNA, and posttranscriptional regulation of translation (14). The employment of a PRF as a mechanism to control the frequency of horizontal transfer has not, to our knowledge, been reported for ICEs or plasmids, but PRF sites are a feature of transposase production by several insertion sequences, where frameshifting is thought to prevent high-frequency transposition that would have a detrimental effect on host survival (28). Several common features of +1 PRF sites have been identified; however, it is clear that individual sites often have distinct features, which could obscure detection from sequence information alone (13, 29, 30). The *msi172* PRF site discovered here differs from other characterized PRF sites and merits further investigation.

mRNA structural elements of PRF sites often promote ribosome stalling, enhancing the chances of slippage between codons. These elements include upstream RBS-like sequences, RNA stem–loop structures, and downstream rare or "hungry" codons encoded by low-concentration tRNAs. For the +1 PRF site of *prfB*, encoding polypeptide chain release factor (RF-2), the mRNA encodes an RBS-like sequence, AGG.GGGU, found 2 bp upstream of the *prfB* frameshift site, which promotes stalling and destabilization of the engaged 0 reading frame (31). The TGG.GGG sequence upstream of the *msi172* PRF resembles an RBS sequence and is conserved in all *msi172* homologs in which a PRF site was identified; however, it is positioned 3 bp further upstream of the slippery codon than the RBS-like site in *prfB*, and, although it possibly promotes stalling, it cannot destabilize the ribosomal complex by the same mechanism as *prfB*. Increasing the distance between the RBS-like sequence and the slippery codon markedly reduces frameshifting (32, 33). Moreover, the amino acid sequence WG can only be specified by the codons TGG.GGN, raising the possibility that the sequence conservation reflects selection at the amino acid level. Hence, the involvement of the sequence in the mechanism or regulation of the PRF remains an open question.

A well-conserved feature of many characterized PRF sites is the presence of a slippery sequence of variable length [for example, the heptanucleotide (X).XXY.YYZ in eukaryotic/viral −1 frameshift sites (34)], where two ribosome-bound charged tRNAs can transition to a compatible codon in an adjacent reading frame. It is less well defined at some +1 frameshift sites, such as the UCC.UGA motif for mammalian antizyme (27) and the CUU.UGA motif of *prfB* (35). Although UUU.YNN consecutive codons are common in PRF sites, they are underrepresented in strongly expressed genes (15–17), possibly due to their propensity to induce ribosome slippage. The wobble position of the tRNA^{phe} anticodon sequence GAA may weaken the interaction of tRNA^{phe} with the UUU codon, promoting movement to the adjacent codon. Consistent with the role of the UUC as the landing position of tRNA^{phe} after the PRF, mutation of the UUU.CGC sequence to UUC.CGC or UUU.AGG abolished the ability of *msi172–msi171* to activate the *rdfS* promoter.

The FseA protein is encoded on a widespread family of proteobacterial ICEs with transfer systems related to those of ICE*Ml*Sym^{R7A} and Tn*4371* (9, 10, 12, 36, 37). The Msi171 portion of FseA is a member of the "domain of unknown function" DUF2285 superfamily (COG5419, pfam10074), with 291 annotated members as of December 2014 (38). Neither the DUF2285 domain nor the *msi172*-encoded portion of FseA shows primary sequence similarity to known DNA-binding proteins. Nevertheless, our experiments demonstrated that FseA activated the *rdfS* promoter in the absence of ICE*Ml*Sym^{R7A}. FseA does not activate at a posttranscriptional level, because *rdfS* promoter activation was achieved in the absence of the *rdfS* coding sequence. QseM also has weak similarity to the DUF2285 family, but, unlike the majority of homologs, it lacks an N-terminal region similar to Msi172. Thus, our data indicate that members of the DUF2285 can participate in both transcriptional activator and antiactivator interactions. Interestingly, a highly conserved DUF2285 homolog is encoded adjacent to the QS (39) and temperature-dependent (40) type VI secretion system (T6SS-4) present in *Yersinia* species. Although the protein-coding capacity of this region has not been investigated, the region has been directly implicated in the regulation of T6SS-4 expression (39, 41, 42).

QseM prevents QS-mediated activation of ICE*Ml*Sym^{R7A} excision and transfer by binding TraR (10), analogous to the mechanism of inhibition of Ti and pRL1JI plasmid transfer by the TraM-family antiactivators (43–45). TraM binds the DNA-binding domain of TraR on the opposite side of the DNA-binding surface (46, 47). More recently, structural characterization of the LasR-binding antiactivator QslA of *Pseudomonas aeruginosa* (48) revealed that in contrast to TraM, QslA binds the ligand-binding domain of LasR (48). Thus, antiactivators of LuxR-family regulators have evolved multiple times and can operate through distinct mechanisms. QseM shows no primary sequence similarity to either of these antiactivators and appears to differ mechanistically to TraM (49) in that it only interacts with TraR in the presence of AHL (10). In this work, we demonstrated that QseM is also able to bind and inhibit the activator of *rdfS* expression FseA. FseA shows no obvious primary sequence similarity to *M. loti* TraR or any other LuxR-family regulator, although it is possible that QseM recognizes secondary

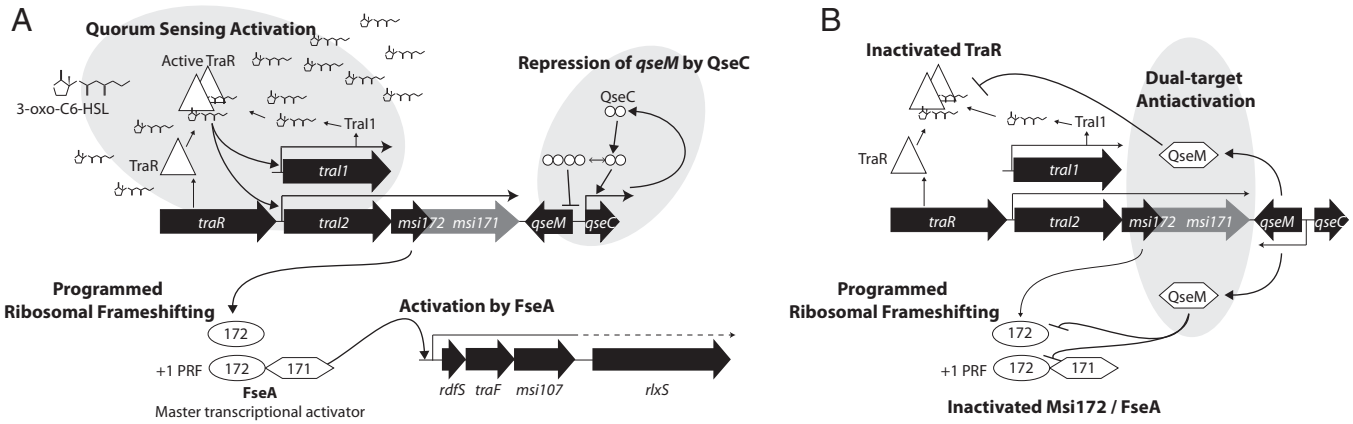

Fig. 3. Model for activation or repression of QS, excision, and transfer of ICE*Ml*Sym^{R7A}. (*A*) In cells that are repressed for *qseM* expression by QseC (10), TraR complexed with *N*-(3-oxo-hexanoyl)-L-homoserine lactone (3-oxo-C6-HSL) activates expression from the *traI1* promoter and from the promoter of *traI2–msi172–msi171* (11). This activation leads to increased production of 3-oxo-C6-HSL, as observed in strain R7AΔ*qseM* (10). Increased transcription of *traI2–msi172–msi171* leads to increased translation of *msi172–msi171*. In 3.9–12.8% of translation events (Fig. 1*C* and Fig. S4), a PRF event occurs, resulting in the production of the master activator FseA. FseA activates transcription from the *rdfS* promoter, resulting in increased expression of the excisionase RdfS, the prepilin protease TraF, and the predicted murein hydrolase Msi107 (9). It remains unknown whether expression of other ICE*Ml*Sym^{R7A} transfer genes including *rlxS* (dotted line) is also activated. In the absence of *qseM*, activation by FseA leads to excision in 40–100% of cells (depending on growth phase) and a 1,000-fold increase in conjugative transfer (10). (*B*) In cells that contain insufficient QseC to repress *qseM* expression (10), QseM is expressed and interacts with TraR–3-oxo-C6-HSL, inhibiting transcription of *traI1*, 3-oxo-C6-HSL production, and transcription of *traI2–msi172–msi171* (11). QseM also binds FseA (Fig. 2), preventing any activation of the *rdfS* promoter that might result from leaky expression of *traI2–msi172–msi171*.

structural elements common to both these proteins. Another possibility is that QseM has evolved as a DNA mimic (50) and is able to interfere with FseA and TraR through interaction with their DNA-binding regions. Alternatively, QseM may have evolved distinct sites with which it binds FseA and TraR, in which case a single QseM molecule may be able to inhibit FseA and TraR simultaneously.

Given that the suppression of ICE*Ml*Sym^{R7A} excision and transfer is so robust, how does ICE*Ml*Sym^{R7A} activate transfer? In laboratory cultures of wild-type *M. loti* R7A, excision of ICE*Ml*Sym^{R7A} occurs in ∼0.06% of cells in log-phase cultures and ∼6% of cells in stationary phase. In strains carrying mutations in *msi172* or *msi171*, excision occurs only sporadically, regardless of growth phase, and transfer is abolished (11). Therefore, expression of FseA is high enough in 6% of cells in stationary-phase cultures to stimulate excision. Given the multiple levels of repression exerted by QseM and the PRF, it is clear that *qseM* expression must be repressed in these cells. Expression of *qseM* is controlled by QseC, a DNA-binding protein that activates its own expression and represses *qseM* expression. As previously proposed (10), the molecular switch comprising QseC and its operator sequences likely facilitates bimodal induction of *qseM*, so that individual cells are either on or off for both QS and excision (Fig. 3). This system may facilitate a bet-hedging strategy by ICE*Ml*Sym^{R7A}, in which only a small proportion of cells in the population can respond to AHL and act as donors for transfer. It remains to be seen whether there are environmental or physiological stimuli that augment the proportion of cells to enter this state, much like the starvation-induced bet-hedging strategy that controls DNA competence and sporulation pathways in *Bacillus subtilis* (51, 52). Given the roles of amino acid starvation in both regulation of plant symbiosis (53) and ribosomal frameshifting (54), and the stationary-phase induction of ICE*Ml*Sym^{R7A} excision (9), we anticipate that nutrient availability likely contributes a critical role in this regulation.

Methods

Strains, Plasmids, and Growth Conditions. Strains and plasmids are listed in Table S3, and plasmid construction is described in *SI Methods*. Primers used for plasmid construction, PCR, RT-PCR, 5′ RACE, and quantitative PCR are listed in Table S4. *E. coli* was cultured on solid or liquid LB medium supplemented with antibiotics to maintain plasmids, and *M. loti* was cultured on solid Rhizobium-defined medium supplemented with glucose (G/RDM), vitamins, and appropriate antibiotics or in tryptone-yeast (TY) liquid culture without antibiotics as described (9, 11, 55). Plasmids introduced into *M. loti* were first introduced into *E. coli* ST18 [supplemented with 5-aminolevulinic acid (56)] and then transferred from ST18 by conjugation.

5′ RACE. RNA from R7AΔ*qseM* was used for 5′ RACE, which was carried out by using the Roche 5′/3′ second-generation kit as described (10, 11). Targeted cDNA synthesis was carried out by using primer 24, and specific amplification of *rdfS* cDNA was carried out first by using primer 25 (SP1) and then primer 26 (SP2), and the resulting product was sequenced by using primer 26.

β-Galactosidase Assays. For assays in Fig. S3, broths inoculated from single colonies of *M. loti* R7ANS cells carrying pSDrdfS–lacZ and derivatives were grown for 72 h. Fresh broths containing 0.1 mM IPTG were inoculated from these cultures (1/100 dilution) and grown for 24 h. Cell density was estimated by OD_{600}, and cells were analyzed for β-galactosidase expression by using the fluorescent substrate 4-methylumbelliferyl β-D-galactoside (MUG) and a Tecan Infinite 200 PRO plate reader, as described (10, 57). For assays in Fig. S4, broths containing 0.4% glucose and 100 μg/mL ampicillin were inoculated from single colonies of *E. coli* cells carrying pUC19 and minimal PRF region derivatives. These cultures were diluted 1/10 into LB containing 1 mM IPTG and 100 μg/mL ampicillin and grown for 24 h. Cell density was estimated by absorbance at 600 nm of 100 μL of culture in an Enspire Multimode Plate Reader (PerkinElmer), and β-galactosidase activity was measured by using the MUG fluorescent assay in the same plate reader (10, 57).

LTQ Orbitrap Mass Spectrometry of MBP Fusion Proteins. MBP fusion proteins were purified by using amylose affinity chromatography, and protein bands from reducing SDS/PAGE gels were excised and digested with trypsin in gel as described (58). Peptides were analyzed by nanoflow liquid chromatography-coupled tandem mass spectrometry, using an Ultimate3000 uHPLC system inline coupled to the nanospray source of a LTQ Orbitrap mass spectrometer (Thermo Scientific). Spectra were searched against a custom sequence database containing predicted peptides that could be produced following a PRF at any nucleotide position downstream of the A437 trypsin site. Detailed protocols of purification and mass spectrometry are provided in *SI Methods*.

Bacterial Two-Hybrid Assays. Bacterial two-hybrid assays were performed by using the Bacteriomatch II system (Agilent) as described (10). Positive protein–protein interactions were detected by increased colony numbers on medium containing 3-amino-1,2,4-triazole compared with numbers on nonselective medium, which provided an estimate of plasmid coelectroporation efficiency (Table S2). Assays were also spotted on selective medium to give a visual representation of the interaction (Fig. 2).

ACKNOWLEDGMENTS. This work was supported by a University of Otago (UOO) Research Grant and a Dean's Bequest consumables grant from the Otago School of Medical Sciences. J.P.R. was supported by a UOO Division of Health Sciences for a Career Development Postdoctoral Fellowship. J.P.R. also acknowledges the Curtin University Faculty of Health Sciences for support of work contributed at Curtin University by himself and students J.R.P.-H. and D.A.H. In addition, J.P.R. received technical support from the Curtin University Curtin Health Innovation Research Institute Biosciences Precinct facility. M.F.H. was supported by a Natural Sciences and Engineering Research Council of Canada Discovery grant.

1. Guglielmini J, Quintais L, Garcillán-Barcia MP, de la Cruz F, Rocha EP (2011) The repertoire of ICE in prokaryotes underscores the unity, diversity, and ubiquity of conjugation. *PLoS Genet* 7(8):e1002222.
2. Burrus V, Pavlovic G, Decaris B, Guédon G (2002) Conjugative transposons: The tip of the iceberg. *Mol Microbiol* 46(3):601–610.
3. Wozniak RA, Waldor MK (2010) Integrative and conjugative elements: Mosaic mobile genetic elements enabling dynamic lateral gene flow. *Nat Rev Microbiol* 8(8):552–563.
4. Sullivan JT, Brown SD, Yocum RR, Ronson CW (2001) The bio operon on the acquired symbiosis island of *Mesorhizobium* sp. strain R7A includes a novel gene involved in pimeloyl-CoA synthesis. *Microbiology* 147(Pt 5):1315–1322.
5. Sullivan JT, et al. (2002) Comparative sequence analysis of the symbiosis island of *Mesorhizobium loti* strain R7A. *J Bacteriol* 184(11):3086–3095.
6. Wyndham RC, Cashore AE, Nakatsu CH, Peel MC (1994) Catabolic transposons. *Biodegradation* 5(3-4):323–342.
7. Sullivan JT, Patrick HN, Lowther WL, Scott DB, Ronson CW (1995) Nodulating strains of *Rhizobium loti* arise through chromosomal symbiotic gene transfer in the environment. *Proc Natl Acad Sci USA* 92(19):8985–8989.
8. Sullivan JT, Ronson CW (1998) Evolution of rhizobia by acquisition of a 500-kb symbiosis island that integrates into a phe-tRNA gene. *Proc Natl Acad Sci USA* 95(9): 5145–5149.
9. Ramsay JP, Sullivan JT, Stuart GS, Lamont IL, Ronson CW (2006) Excision and transfer of the *Mesorhizobium loti* R7A symbiosis island requires an integrase IntS, a novel recombination directionality factor RdfS, and a putative relaxase RlxS. *Mol Microbiol* 62(3):723–734.
10. Ramsay JP, et al. (2013) A widely conserved molecular switch controls quorum sensing and symbiosis island transfer in *Mesorhizobium loti* through expression of a novel antiactivator. *Mol Microbiol* 87(1):1–13.
11. Ramsay JP, et al. (2009) A LuxRI-family regulatory system controls excision and transfer of the *Mesorhizobium loti* strain R7A symbiosis island by activating expression of two conserved hypothetical genes. *Mol Microbiol* 73(6):1141–1155.
12. Toussaint A, et al. (2003) The biphenyl- and 4-chlorobiphenyl-catabolic transposon Tn*4371*, a member of a new family of genomic islands related to IncP and Ti plasmids. *Appl Environ Microbiol* 69(8):4837–4845.
13. Antonov I, Coakley A, Atkins JF, Baranov PV, Borodovsky M (2013) Identification of the nature of reading frame transitions observed in prokaryotic genomes. *Nucleic Acids Res* 41(13):6514–6530.
14. Baranov PV, Gesteland RF, Atkins JF (2002) Recoding: Translational bifurcations in gene expression. *Gene* 286(2):187–201.
15. Fox TD, Weiss-Brummer B (1980) Leaky +1 and -1 frameshift mutations at the same site in a yeast mitochondrial gene. *Nature* 288(5786):60–63.
16. Atkins JF, Nichols BP, Thompson S (1983) The nucleotide sequence of the first externally suppressible—1 frameshift mutant, and of some nearby leaky frameshift mutants. *EMBO J* 2(8):1345–1350.
17. Schwartz R, Curran JF (1997) Analyses of frameshifting at UUU-pyrimidine sites. *Nucleic Acids Res* 25(10):2005–2011.
18. Crooks GE, Hon G, Chandonia JM, Brenner SE (2004) WebLogo: A sequence logo generator. *Genome Res* 14(6):1188–1190.
19. Svenningsen SL, Costantino N, Court DL, Adhya S (2005) On the role of Cro in lambda prophage induction. *Proc Natl Acad Sci USA* 102(12):4465–4469.
20. Bergstrom CT, Lipsitch M, Levin BR (2000) Natural selection, infectious transfer and the existence conditions for bacterial plasmids. *Genetics* 155(4):1505–1519.
21. Levin BR, Bergstrom CT (2000) Bacteria are different: Observations, interpretations, speculations, and opinions about the mechanisms of adaptive evolution in prokaryotes. *Proc Natl Acad Sci USA* 97(13):6981–6985.
22. Harrison E, Brockhurst MA (2012) Plasmid-mediated horizontal gene transfer is a coevolutionary process. *Trends Microbiol* 20(6):262–267.
23. Mruk I, Kobayashi I (2014) To be or not to be: Regulation of restriction-modification systems and other toxin-antitoxin systems. *Nucleic Acids Res* 42(1):70–86.
24. Goryachev AB (2011) Understanding bacterial cell-cell communication with computational modeling. *Chem Rev* 111(1):238–250.
25. Goryachev AB, et al. (2005) Transition to quorum sensing in an *Agrobacterium* population: A stochastic model. *PLOS Comput Biol* 1(4):e37.
26. Gesteland RF, Weiss RB, Atkins JF (1992) Recoding: Reprogrammed genetic decoding. *Science* 257(5077):1640–1641.
27. Poole ES, Major LL, Cridge AG, Tate WP (2006) The mechanism of recoding in pro- and eukaryotes. *Protein Synthesis and Ribosome Structure*, eds Nierhaus KH, Wilson DN (Wiley-VCH, Weinheim, Germany), pp 397–428.
28. Chandler M, Fayet O (1993) Translational frameshifting in the control of transposition in bacteria. *Mol Microbiol* 7(4):497–503.
29. Bekaert M, et al. (2010) Recode-2: New design, new search tools, and many more genes. *Nucleic Acids Res* 38(Database issue):D69–D74.
30. Sharma V, et al. (2011) A pilot study of bacterial genes with disrupted ORFs reveals a surprising profusion of protein sequence recoding mediated by ribosomal frameshifting and transcriptional realignment. *Mol Biol Evol* 28(11):3195–3211.
31. Márquez V, Wilson DN, Tate WP, Triana-Alonso F, Nierhaus KH (2004) Maintaining the ribosomal reading frame: The influence of the E site during translational regulation of release factor 2. *Cell* 118(1):45–55.
32. Weiss RB, Dunn DM, Atkins JF, Gesteland RF (1987) Slippery runs, shifty stops, backward steps, and forward hops: -2, -1, +1, +2, +5, and +6 ribosomal frameshifting. *Cold Spring Harb Symp Quant Biol* 52:687–693.
33. Devaraj A, Fredrick K (2010) Short spacing between the Shine-Dalgarno sequence and P codon destabilizes codon-anticodon pairing in the P site to promote +1 programmed frameshifting. *Mol Microbiol* 78(6):1500–1509.
34. Gale M, Jr, Tan SL, Katze MG (2000) Translational control of viral gene expression in eukaryotes. *Microbiol Mol Biol Rev* 64(2):239–280.
35. Craigen WJ, Caskey CT (1986) Expression of peptide chain release factor 2 requires high-efficiency frameshift. *Nature* 322(6076):273–275.
36. Ryan MP, Pembroke JT, Adley CC (2009) Novel Tn*4371*-ICE like element in *Ralstonia pickettii* and genome mining for comparative elements. *BMC Microbiol* 9:242.
37. Ohtsubo Y, et al. (2012) Conjugal transfer of polychlorinated biphenyl/biphenyl degradation genes in *Acidovorax* sp. strain KKS102, which are located on an integrative and conjugative element. *J Bacteriol* 194(16):4237–4248.
38. Finn RD, et al. (2014) Pfam: The protein families database. *Nucleic Acids Res* 42(Database issue):D222–D230.
39. Zhang W, et al. (2011) Modulation of a thermoregulated type VI secretion system by AHL-dependent quorum sensing in *Yersinia pseudotuberculosis*. *Arch Microbiol* 193(5):351–363.
40. Pieper R, et al. (2009) Temperature and growth phase influence the outer-membrane proteome and the expression of a type VI secretion system in *Yersinia pestis*. *Microbiology* 155(Pt 2):498–512.
41. Gueguen E, et al. (2013) Expression of a Yersinia pseudotuberculosis Type VI Secretion System Is Responsive to Envelope Stresses through the OmpR Transcriptional Activator. *PLoS ONE* 8(6):e66615.
42. Zhang W, et al. (2013) A type VI secretion system regulated by OmpR in *Yersinia pseudotuberculosis* functions to maintain intracellular pH homeostasis. *Environ Microbiol* 15(2):557–569.
43. Danino VE, Wilkinson A, Edwards A, Downie JA (2003) Recipient-induced transfer of the symbiotic plasmid pRL1JI in *Rhizobium leguminosarum* bv. *viciae* is regulated by a quorum-sensing relay. *Mol Microbiol* 50(2):511–525.
44. Fuqua C, Burbea M, Winans SC (1995) Activity of the *Agrobacterium* Ti plasmid conjugal transfer regulator TraR is inhibited by the product of the *traM* gene. *J Bacteriol* 177(5):1367–1373.
45. Qin Y, Su S, Farrand SK (2007) Molecular basis of transcriptional antiactivation. TraM disrupts the TraR-DNA complex through stepwise interactions. *J Biol Chem* 282(27): 19979–19991.
46. Chen G, Jeffrey PD, Fuqua C, Shi Y, Chen L (2007) Structural basis for antiactivation in bacterial quorum sensing. *Proc Natl Acad Sci USA* 104(42):16474–16479.
47. Vannini A, Volpari C, Di Marco S (2004) Crystal structure of the quorum-sensing protein TraM and its interaction with the transcriptional regulator TraR. *J Biol Chem* 279(23):24291–24296.
48. Fan H, et al. (2013) QsIA disrupts LasR dimerization in antiactivation of bacterial quorum sensing. *Proc Natl Acad Sci USA* 110(51):20765–20770.
49. Luo ZQ, Qin Y, Farrand SK (2000) The antiactivator TraM interferes with the autoinducer-dependent binding of TraR to DNA by interacting with the C-terminal region of the quorum-sensing activator. *J Biol Chem* 275(11):7713–7722.
50. Wang HC, Ho CH, Hsu KC, Yang JM, Wang AH (2014) DNA mimic proteins: Functions, structures, and bioinformatic analysis. *Biochemistry* 53(18):2865–2874.
51. Schultz D, Wolynes PG, Ben Jacob E, Onuchic JN (2009) Deciding fate in adverse times: Sporulation and competence in *Bacillus subtilis*. *Proc Natl Acad Sci USA* 106(50): 21027–21034.
52. Veening JW, et al. (2008) Bet-hedging and epigenetic inheritance in bacterial cell development. *Proc Natl Acad Sci USA* 105(11):4393–4398.
53. Prell J, et al. (2010) Role of symbiotic auxotrophy in the *Rhizobium*-legume symbioses. *PLoS ONE* 5(11):e13933.
54. Xie P (2014) Dynamics of +1 ribosomal frameshifting. *Math Biosci* 249:44–51.
55. Ronson CW, Nixon BT, Albright LM, Ausubel FM (1987) *Rhizobium meliloti ntrA* (*rpoN*) gene is required for diverse metabolic functions. *J Bacteriol* 169(6):2424–2431.
56. Thoma S, Schobert M (2009) An improved *Escherichia coli* donor strain for diparental mating. *FEMS Microbiol Lett* 294(2):127–132.
57. Ramsay JP (2013) High-throughput β-galactosidase and β-glucuronidase Assays Using Fluorogenic Substrates. *Bio-protocol* 3(14):e827.
58. Shevchenko A, et al. (1996) Linking genome and proteome by mass spectrometry: Large-scale identification of yeast proteins from two dimensional gels. *Proc Natl Acad Sci USA* 93(25):14440–14445.